

Structural and electronic transitions in the low-temperature, high-pressure phase of SmS

P. P. Deen,¹ D. Braithwaite,² N. Kernavanois,^{3,1} L. Paolasini,¹ S. Raymond,² A. Barla,^{2,1} G. Lapertot,² and J. P. Sanchez²¹European Synchrotron Radiation Facility, B.P. 220, F-38043 Grenoble, France²Département de Recherche Fondamentale sur la Matière Condensée, SPSMS, CEA Grenoble, F-38054 Grenoble, France³Institut Laue Langevin, B.P. 156, F-38042, Grenoble, France

(Received 24 February 2005; published 30 June 2005)

Structural and electronic properties of samarium sulfide were studied under pressure up to 2.9 GPa and at low temperatures down to 4.5 K via x-ray diffraction and absorption techniques. The measurements are a direct probe of the valence and structural state of samarium sulphide at low temperatures through the black-to-gold and magnetic transitions. A divalent state is found below the first-order valence transition reached in this study at 58 K and 1.13 GPa. Above the transition, the valence increases linearly with pressure. In particular, it is found the samarium has an intermediate valence [2.81 (4)] in the magnetically ordered phase at 2.9 GPa and 4.5 K. Resonant x-ray magnetic scattering found no evidence of type I or type IA magnetic order in the magnetically ordered phase.

DOI: 10.1103/PhysRevB.71.245118

PACS number(s): 71.20.Eh, 61.50.Ks, 62.50.+p

Recent years have seen the resurgence of interest in the behavior of strongly correlated electron systems. Particular emphasis has been placed on the issues of spin and charge fluctuations close to a magnetic instability in mixed valence systems. The most remarkable breakthrough was the discovery of superconductivity close to the magnetic quantum critical point of several heavy fermion systems.¹ The interaction responsible for this nonconventional superconducting state is generally attributed to spin fluctuations though charge fluctuations may also play a role. In fact it is suspected that charge fluctuations enhance the superconductivity in several of these systems.² The classical intermediate-valence system SmS provides an ideal opportunity to study charge fluctuations in the vicinity of a magnetic quantum-critical point.

At ambient pressure SmS is a semiconductor that crystallizes in the NaCl structure with divalent, or close to divalent, Sm.³ A small increase in pressure (0.65 GPa) at room temperature is sufficient to induce a well-known volume collapse of about 15%.⁴ This first-order isostructural phase transition alters the valence state of Sm to a homogenous intermediate-valent state⁴⁻⁶ and the color of the sample from black to gold. In the high-pressure (gold) phase, the high-temperature resistivity is metallic but on lowering the temperature a crossover to a strongly correlated semiconductor is observed. This is only suppressed with pressures above ~ 2.0 GPa.^{7,8} The phase diagram for SmS is presented in Fig. 1.

It is difficult to access the black-to-gold transition at low temperatures. This is mainly due to the first-order nature of the transition and the strong hysteresis, which means that the transition can only be determined by *in situ* pressure changes at low temperature. In fact, there are very few measurements of the black-to-gold transition pressure at low temperature. McWhan *et al.*¹¹ performed a single measurement on the lattice parameter at 85 K where the pressure was increased *in situ*. They concluded that the transition pressure is increased by only 0.1 GPa in comparison to the 300 K value, although the maximum pressure reached (0.8 GPa) was not sufficient to obtain a complete high-pressure phase. Further information on the black-to-gold transition has been gained by resis-

tivity measurements.^{6,9,13} The determination of the transition pressure from the resistivity is not obvious and this led Morillo *et al.*⁹ and Bader *et al.*⁶ to extract very different values using the same data set. Any other results have been obtained in experiments where the pressure was fixed at ambient temperature before cooling. In these cases the sample remained in the high-pressure phase upon cooling because of the strong hysteresis. As a result of these difficulties the phase diagram, as the black-to-gold transition is crossed, is as yet not well established. The contribution of this study to the phase diagram will be discussed more fully in the latter part of this paper.

The phase diagram also shows the magnetic transition T_M established by very recent nuclear forward scattering (NFS) and specific heat measurements under high pressure. These measurements unambiguously show the onset of long-range magnetic order at 2.0 GPa.^{12,14} It was always expected that

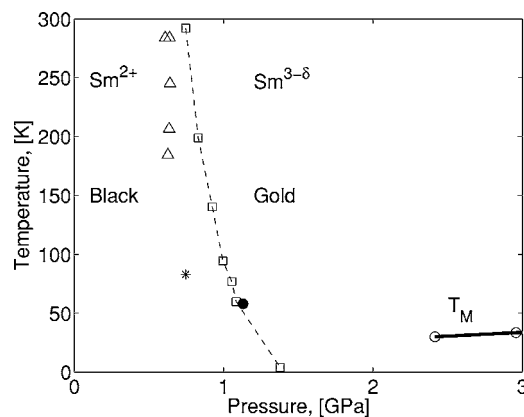


FIG. 1. The phase diagram for SmS showing different measurements of the phase boundary between the black semiconducting and golden metallic phases. \square data sets obtained by Morillo *et al.*⁹ The broken line is a guide to the eye. The \triangle represents data reported by Ref. 10, the * is as reported by McWhan *et al.*, Ref. 11, and the \circ shows the magnetic transition,¹² \bullet represents this work. T_M denotes the magnetic transition.

SmS would reach a trivalent state upon the application of sufficiently high pressure and that long-range magnetic order should exist since Sm^{3+} is a Kramers ion.¹⁵ In fact it has generally been accepted that long-range magnetic order in Sm compounds can only be obtained when the trivalent Sm^{3+} state is reached. However, recent band-structure calculations suggest that the intermediate-valent state of Sm could sustain a nonzero magnetic moment.¹⁶ High-pressure x-ray absorption studies on SmS at room temperature were performed more than 20 years ago¹⁷ and show a valence of 2.6 at the volume collapse, which increases to ~ 2.65 at 2.0 GPa. There are, to date, no measurements of the valence of Sm at low temperatures. It is therefore uncertain whether the magnetic state at low temperatures coexists with intermediate or trivalent Sm.

The aim of this work is to further establish the SmS (p , T) phase diagram in terms of the structural and valence transitions and their association with the semiconductor to metal and magnetic transitions. This is achieved via absorption spectra and x-ray diffraction under these pressures and temperature conditions where magnetic order occurs. These spectra reflect the valence state of Sm in SmS as the black-to-gold transition is crossed and as magnetic order emerges. Furthermore, systematic measurements on the lattice parameters allows the correlation of the structure with the valence state and magnetic order. A discontinuous volume contraction is expected as magnetic order emerges with a valence jump toward a trivalent state.¹⁴

This work has been performed on the magnetic-scattering beamline ID20 at the European Synchrotron Radiation Facility. Single-crystal SmS samples have been grown using the Bridgman technique in a sealed Tantalum crucible and thereafter cleaved to obtain the required dimensions $60 \mu\text{m} \times 110 \mu\text{m} \times 280 \mu\text{m}$. The $[0\ 0\ 1]$ scattering plane was employed since platelets with this orientation are easily cleaved in SmS. Other orientations would require polishing, and this can be sufficient to induce the transition to the high-pressure phase on the surface.

Hydrostatic pressure was applied using a Moissanite anvil cell adapted for use under x-ray-scattering conditions at low temperatures. The incident and exit scattering paths are through a Be gasket, 0.25 mm thick, with external and internal diameters of 2 and 1 mm, respectively. Low-energy x rays, 3–10 keV, can therefore be scattered without severe absorption along the scattering path. The pressure-transmitting medium was nitrogen. The sample was mounted in a variable temperature cryostat (1.5–300 K) with an insert capable of *in situ* pressure changes and measurements. To determine the pressure transmitted to the sample the ruby fluorescence technique was employed thereby monitoring the pressure directly at each pressure change with an average uncertainty of 0.03 GPa. A more detailed description of the experimental setup will be published elsewhere.¹⁸

The pressure was initially increased at 4.5 K in three steps up to 0.73 GPa. However, mechanical complications made it difficult to further increase the pressure at this temperature. Subsequent pressure steps required heating the pressure cell to progressively higher temperatures in the range 50–100 K. Once the expected pressure was obtained it was possible to cool the sample to 4.5 K without significant loss of pressure.

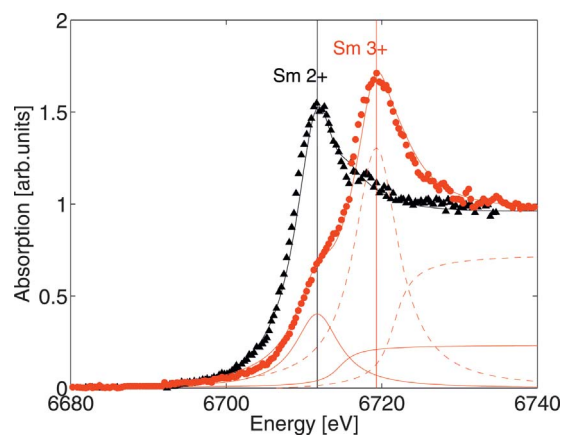


FIG. 2. (Color) Absorption spectra around the Sm L_{III} edge for pressures $p=0$ GPa and $p=1.85$ GPa at 4.5 K. The position of the Sm^{2+} and Sm^{3+} white line peaks are indicated. The Lorentzian and arctan functions represent Eq. (1) used to determine the valence state of Sm. The full black and red lines through the absorption spectra are fits to the ambient-pressure and high-pressure data, respectively.

Pressures up to 2.86 GPa at 4.5 K were reached in this manner. Under these conditions absorption, in fluorescence yield mode, and x-ray-diffraction measurements have been performed around the Sm L_{III} absorption edge, $E=6716$ eV, with an energy resolution of $\Delta E/E=10^{-4}$.

The valence state, derived from absorption spectra, was obtained over the complete pressure range, 0–2.86 GPa, and also at temperatures 4.5 and 50 K. Therefore it was also possible to determine the valence variation with temperature. These data provide the first direct measurements of the valence state of Sm in the magnetically ordered state of SmS.

Figure 2 displays the absorption spectra of the black and gold phases at 4.5 K. The raw fluorescence spectra were normalized to the incident-beam monitor and thereafter were normalized with respect to the intensities below and above the white line. The intensities below the white line were used to perform a background subtraction. The high-energy data were used to normalize the data set to unity above the white line. Therefore, the background below the white line corresponds to zero excitations and those above to unity. A self-absorption correction in accordance with¹⁹ was furthermore applied to finally obtain the absorption spectra. The spectrum at 0 GPa clearly reveals a single white line indicative of the divalent state at 6711.7 eV. Alternatively, the spectrum obtained at 1.85 GPa displays two white lines at 6711.7 and 6719.3 eV corresponding to the divalent and trivalent states, respectively, representative of the intermediate valence state.

Figure 3 shows the change in the absorption line shape on the application of pressure in the gold phase at 4.5 K. The trivalent white line is dominant across the gold phase with a reduction in the intensity of the divalent white line as the pressure is increased. Nevertheless, the Sm^{2+} white line remains as a shoulder beyond 2.0 GPa where magnetism has been implied. In fact, this shoulder is still present at 2.86 GPa, indicating that Sm has not entered its trivalent state. Long-range magnetic order has therefore been implied, con-

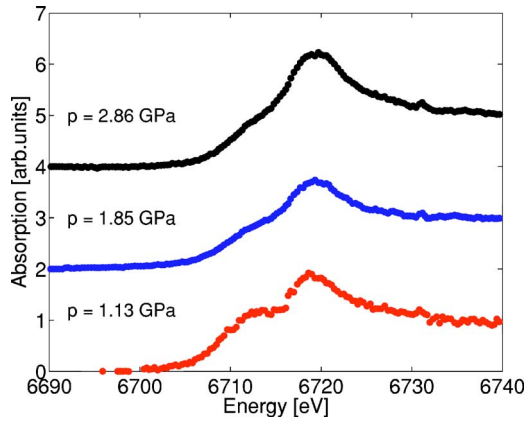


FIG. 3. (Color online) Absorption spectra with increasing pressure above the semiconductor to metal transition at $T=4.5$ K. The low-energy shoulder corresponds to the white line of Sm^{2+} and has not disappeared by 2.86 GPa, ~ 0.9 GPa above the pressure where magnetic order has been implied.

trary to expectation, with Sm in its intermediate-valent state.

The spectrum of a mixed-valent atomic state has characteristic structure because of the existence of two white lines corresponding to the integer valent states, $4f^n$ and $4f^{n+1}$. The absorption line shapes have been analyzed using Lorentzian and arctangent functions to represent the excitation and a continuous background, respectively, for both integer valent states, Sm^{2+} and Sm^{3+} .²⁰ Using the simplex Nelder-Mead method of least-squares fitting,²¹ a fit of the parameters in the following expression was performed:

$$I(E) = B_0 + B_1 E + \sum_{k=1,2} \frac{p(k)\Gamma^2}{\Gamma^2 + (E - E_k)^2} + \sum_{c=1,2} \frac{p(c)}{p(1) + p(2)} \left(0.5 + \frac{1}{\pi} \text{atan} \left[\frac{E - (E_c + \delta)}{0.5\Gamma} \right] \right). \quad (1)$$

In this expression E denotes the energy with $B_0 + B_1 E$ representing a linear background. The L_{III} absorption edge of the Lanthanides mainly gives rise to an excitation from a $2p$ core electron to an empty state in the $5d$ conduction band. This excitation can be modeled using a Lorentzian with a half-width at full maximum, Γ , representative of the core-hole lifetime. The strengths of the individual Lorentzian line shapes are given by p_1 and p_2 . The background continuum denotes any excitation above the first ionization potential. In Sm this is 5.6 eV above the point of inflexion of the absorption line shapes and so $E_c = 6714.6$ and 6721.6 for the di- and trivalent lines, respectively. The δ value denotes a slight shift of the continuum of -1.6 eV as observed in metallic systems.²⁰ The white lines occur at $E_1 = 6711.7$ and $E_2 = 6719.3$ eV. A fit of the absorption line shapes indicated that $\Gamma = 3.4(2)$ eV for all the spectra. This is comparable to the value of Γ quoted for Eu, the element adjacent to Sm in the Lanthanides.²⁰ Since Γ is equivalent in both the black and gold phases the matrix elements for the $2p$ - $5d$ excitations, as probed in the rare-earth systems at L absorption edges, are similar in both the divalent and intermediate va-

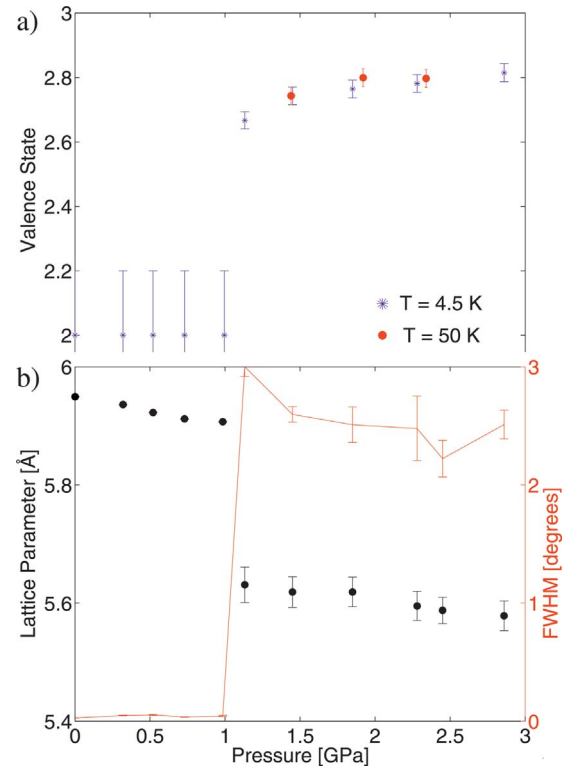


FIG. 4. (Color) (a) Valence state of Sm in SmS obtained by fluorescence spectra for $T=4.5$ and 50 K. (b) Variation of the lattice parameters, obtained from the (0 0 4) Bragg diffraction peak, as a function of pressure with the increase in mosaic spread given on the right-hand y-axis.

lent state. The independent parameters optimized in Eq. (1) were therefore p_1 , p_2 , B_0 , and B_1 . The correlation coefficient for the fits ranged from 0.962 to 0.989. The valence state were then extracted from the relative strengths of the Lorentzian line shapes.

Figure 4(a) shows the valence states of Sm in SmS calculated using Eq. (1). Below the transition a single white line in the absorption spectra indicates a uniquely divalent state. This is not necessarily accurate since analysis of the data reveal that any valence up to 2.2 would appear as divalent. The continuum behind the divalent white line obscures the small contribution of the trivalent white line. Hence, it is not possible to verify the claim by Röhler *et al.*²⁰ that a non-integer valence state exists below the semiconductor to metal transition. Although the variation of the lattice parameter in the black phase [Fig. 4(b)] might indicate an increase in valence via Vegard's lattice parameter analysis, it is impossible to correctly determine this state since this requires the bulk modulus value and the lattice parameter of the trivalent state.²² The first-order phase transition occurred at 58 K and 1.13 GPa and is followed by a linear increase in valence from 2.67(4) at 1.13 GPa to 2.81(4) electrons at 2.86 GPa. The determination of the valence at high pressure is more precise at high pressures since there is no continuum masking the weak contribution of the line. Above 2.0 GPa, where magnetic order occurs in SmS, our measurements clearly show an intermediate valence both above and below the ordering temperature. The pressure variation of the valence

that we find implies that SmS will not become trivalent until at least 6 GPa.

We now discuss the phase diagram of the first-order black-to-gold phase transition. In this study, the lattice parameters were measured at 4.5 K from the (0 0 4) structural Bragg peak. The initial aim was to cross the black-gold boundary at 4.5 K but for reasons described in the experimental section this was unsuccessful. Instead it was necessary to increase the temperature to 58 K in order to attain a pressure of 1.13 GPa and, thus, reach the transition. This provides a new point on the phase diagram (see Fig. 1) and is an indication that the first-order transition is coincident with the analysis of the resistivity measurements by Morillo *et al.*⁹

On crossing the transition an isostructural volume collapse of 13% was observed and although the sample remained a single crystal, the mosaicity increased substantially from 0.030(2)^o to 2.5(1)^o. Below the transition a single Bragg peak was observed corresponding to the black phase. As the transition was crossed two peaks were resolved showing the phase separation within the sample. At higher pressures a single peak remained implying the occurrence of a homogeneous mixed phase. As the pressure is further increased a uniform volume contraction is observed. No discontinuous volume contraction, as expected with the onset of magnetic order with trivalent Sm, was observed. This is in accordance with an intermediate-valence state for Sm.

Barla *et al.*¹² observed magnetic order in SmS using NFS, but this technique is unable to determine the precise magnetic structure. Via resonant x-ray magnetic scattering (RXMS) it is possible to probe the electronic state of the magnetically ordered species and gain spatial information on this magnetic state.²³ The feasibility of RXMS from bulk Sm and Sm compounds has been amply demonstrated.^{24–26} The magnetic order found in rare-earth chalcogenides is typically a type I, II, or IA antiferromagnet.²⁷ A search for magnetic order will therefore commence along the principal symmetry directions. A [0 0 1] scattering plane enables a search for type I and IA structures along the [0 0 L] direction. The large mosaicity of the sample used to determine the valence state hinders the search for a magnetic signal since the deterioration of the sample results in a reduced scattering intensity. A different single crystal sample was therefore cleaved from the same batch with dimensions

80 $\mu\text{m} \times 150 \mu\text{m} \times 300 \mu\text{m}$. In an attempt to preserve the mosaicity the phase transition was crossed at ambient temperature. The mosaicity of the sample was 0.26(5)^o at 1.1 GPa and 300 K. In the magnetic phase, $T=4.5$ K and $p=2.7$ GPa, the mosaicity had increased to 0.8(5)^o, which is substantially lower than the mosaicity observed by crossing the black-to-gold phase transition at low temperatures. In this scattering geometry it is possible to probe for antiferromagnetic wave vectors around (0 0 L) reciprocal space positions. Useful expressions for the scattering amplitudes have been developed by Hannon *et al.*,²⁸ Hamrick,²⁹ Hill and McMorrow,³⁰ and for the particular case of Sm by Stunault *et al.*²⁵ In the case of SmS the resonant magnetic dipole signal of the first harmonic for the (0 0 2.5), (0 0 3), and (0 0 3.5) positions in the π - σ polarization channel is calculated to be $\sim 10^{-5}$ relative to the (0 0 2) charge-scattering intensity. Accordingly an extensive search was performed around the Sm L_{III} absorption edge using a Cu (2 2 0) polarization analyzer crystal to detect RXMS in the π - σ polarization channel. However, no detectable signal was found, leading to the conclusion that long-range magnetic order with $\mathbf{q}=(00L)$ does not exist. This leaves open the possibility of a type II antiferromagnetic structure with $\mathbf{q}=(0.50.50.5)$. Further experiments to search for this magnetic ordering wave vector are anticipated.

A greater understanding of the (p, T) phase diagram of SmS has been gained from fluorescence spectra and x-ray diffraction measurements at the Sm L_{III} absorption edge. In particular, it has been possible to map the valence state of Sm in SmS and the structure of SmS by *in situ* pressure increases at 4.5 K up to 2.86 GPa. The structural and electronic state both undergo a first-order phase transition at 1.13 GPa and 58 K. This data provide the first point on the transition curve by structural measurements and confirms the trend obtained by resistivity measurements.⁹ The electronic state of Sm as magnetic order is established shows no discontinuity and contrary to expectation magnetic order exists with intermediate-valent Sm. The valence state at the onset of magnetic order extracted from this work is 2.78(4). This agrees with the band-structure calculations by Antonov *et al.*¹⁶ where a low-moment magnetic ground state exists in the low-temperature golden phase of SmS with Sm in an intermediate valence state of 2.86.¹⁶

¹N. D. Mathur, F. M. Grosche, S. R. Julian, I. R. Walker, D. M. Freye, R. K. W. Haselwimmer, and G. G. Lonzarich, *Nature* (London) **394**, 39 (1998).

²A. T. Holmes, D. Jaccard, and K. Miyake, *Phys. Rev. B* **69**, 024508 (2004).

³A. Jayaraman, V. Narayanamurti, E. Bucher, and R. G. Maines, *Phys. Rev. Lett.* **25**, 1430 (1970).

⁴M. B. Maple and D. Wohllebe, *Phys. Rev. Lett.* **27**, 511 (1971).

⁵J. M. D. Coey, S. K. Ghatak, M. Avignon, and F. Holtzberg, *Phys. Rev. B* **14**, 3744 (1976).

⁶S. D. Bader, N. E. Phillips, and D. B. McWhan, *Phys. Rev. B* **7**, 4686 (1973).

⁷F. Lapiere, M. Ribault, F. Holtzberg, and J. Flouquet, *Solid State Commun.* **40**, 347 (1981).

⁸F. Holtzberg and J. Wittig, *Solid State Commun.* **40**, 315 (1981).

⁹J. Morillo, M. Konczykowski, and J. P. Senateur, *Valence Instabilities*, edited by P. Wachter (North-Holland, Amsterdam, 1982), p. 151.

¹⁰A. Jayaraman, P. Dernier, and L. D. Longinotti, *Phys. Rev. B* **11**, 2783 (1975).

¹¹D. B. McWhan, S. M. Shapiro, J. Eckert, H. A. Mook, and R. J. Birgeneau, *Phys. Rev. B* **18**, 3623 (1978).

¹²A. Barla, J. P. Sanchez, Y. Haga, G. Lapertot, B. P. Doyle, O. Leupold, R. Ruffer, M. M. Abd-Elmeguid, R. Lengsdorf, and J.

- Flouquet, Phys. Rev. Lett. **92**, 066401 (2004).
- ¹³M. Konczykowski, F. Lapierre, P. Haen, J. Morillo, and J. P. Sénateur, Solid State Commun. **40**, 517 (1981).
- ¹⁴Y. Haga, B. Salce, G. Lapertot, I. Sheikin, K. Matsubayashi, N. K. Sato, J. Flouquet, J. Derr, and A. Barla, Phys. Rev. B **70**, 220406(R) (2003).
- ¹⁵F. Lapierre, M. Ribault, J. Flouquet, and F. Holtzberg, J. Magn. Mater. **31–34**, 443 (1983).
- ¹⁶V. N. Antonov, B. N. Harmon, and A. N. Yaresko, Phys. Rev. B **66**, 165208 (2002).
- ¹⁷J. Röhler, *Handbook on the Physics and Chemistry of Rare Earths*, edited by K. A. Gschneidner, L. Eyring, and S. Hufner (North-Holland, Amsterdam, 1987), Vol. 10, Chap. 71.
- ¹⁸N. Kernavanois (unpublished).
- ¹⁹P. Pfalzer, J. P. Urbach, M. Klemm, S. Horn, M. L. denBoer, A. I. Frenkel, and J. P. Kirkland, Phys. Rev. B **60**, 9335 (1999).
- ²⁰J. Röhler, J. Magn. Mater. **47–48**, 175 (1985).
- ²¹J. A. Nelder and R. Mead, Comput. J. **7**, 308 (1965).
- ²²G. Neumann, R. Pott, J. Röhler, W. Schlabitz, D. Wohlleben, and H. Zahel, *Valence Instabilities*, edited by P. Wachter (North-Holland, Amsterdam, 1982), p. 87.
- ²³M. Blume and D. Gibbs, Phys. Rev. B **37**, 1779 (1988).
- ²⁴D. Watson, E. Forgan, W. Stirling, W. J. Nuttal, S. Perry, M. Costa, and D. Fort, J. Magn. Mater. **140–144**, 743 (1995).
- ²⁵A. Stunault, K. Dumesnil, C. Dufour, C. Vettier, and N. Bernhoeft, Phys. Rev. B **65**, 064436 (2002).
- ²⁶C. Detlefs, A. H. M. Z. Islam, A. I. Goldman, C. Stassis, P. C. Canfield, J. P. Hill, and D. Gibbs, Phys. Rev. B **55**, R680 (1997).
- ²⁷O. Vogt and K. Mattenberger, *Handbook on the Physics and Chemistry of Rare Earths*, edited by K. A. Gschneidner, L. Eyring, G. H. Lander, and G. R. Choppin (North-Holland, Amsterdam, 1993), Vol. 17, p. 301.
- ²⁸J. P. Hannon, G. T. Trammell, M. Blume, and D. Gibbs, Phys. Rev. Lett. **61**, 1245 (1988).
- ²⁹M. Hamrick, Ph.D. thesis, 1994.
- ³⁰J. Hill and D. F. McMorrow, Acta Crystallogr., Sect. A: Found. Crystallogr. **52**, 236 (1996).